NASA TECHNICAL NOTE

NASA TN D-7484

NASA TN D-7484

ISOTHERMAL AND CYCLIC OXIDATION AT 1000° AND 1100° C OF FOUR NICKEL-BASE ALLOYS: NASA-TRW VIA, B-1900, 713C, AND 738X

by Charles A. Barrett, Gilbert J. Santoro, and Carl E. Lowell

Lewis Research Center
Cleveland, Ohio 44135

NATIONAL AERONAUTICS AND SPACE ADMINISTRATION • WASHINGTON, D. C. • NOVEMBER 1973

1. Report No.	2. Government Accession No.	3. Recipient's Catalog No.
NASA TN D-7484		

4. Title and Subtitle	5. Report Date
ISOTHERMAL AND CYCLIC OXIDATION AT 1000° AND 1100° C OF FOUR NICKEL-BASE ALLOYS: NASA-TRW VIA, B-1900, 713C, AND 738X	November 1973
	6. Performing Organization Code
7. Author(s)	8. Performing Organization Report No.
Charles A. Barrett, Gilbert J. Santoro, and Carl E. Lowell	E-7488
	10. Work Unit No.
9. Performing Organization Name and Address	501-01
Lewis Research Center National Aeronautics and Space Administration Cleveland, Ohio 44135	11. Contract or Grant No.
	13. Type of Report and Period Covered
12. Sponsoring Agency Name and Address	Technical Note
National Aeronautics and Space Administration Washington, D.C. 20546	14. Sponsoring Agency Code

15. Supplementary Notes

16. Abstract

The isothermal and cyclic oxidation resistance of four cast Ni-base $\gamma + \gamma'$ alloys, NASA-TRW VIA, B-1900, 713C and 738X, was determined in still air at 1000° and 1100° C. The oxidation process was evaluated by specific sample weight change with time, sample thickness change, X-ray diffraction of the scales, and sample metallography. The behavior is discussed in terms of the Cr, Al, and refractory metal contents of the alloys.

17. Key Words (Suggested by Author(s))	18. Distribution Statement
Superalloys; Nickel base alloys; Isothermal oxidation; Cyclic oxidation; Scaling; Oxide spalling; Aircraft gas turbine alloys; NiCrAl alloys; Refractory metal alloy additions	Unclassified - unlimited

19. Security Classif. (of this report)	20. Security Classif. (of this page)	21. No. of Pages	22. Price*
Unclassified	Unclassified	34	Domestic, $3.00 Foreign, $5.50

* For sale by the National Technical Information Service, Springfield, Virginia 22151

ISOTHERMAL AND CYCLIC OXIDATION AT 1000° AND 1100° C OF FOUR NICKEL-BASE ALLOYS: NASA-TRW VIA, B-1900, 713C, AND 738X

by Charles A. Barrett, Gilbert J. Santoro, and Carl E. Lowell

Lewis Research Center

SUMMARY

Four cast $\gamma + \gamma'$ nickel-base alloys, NASA-TRW VIA, B-1900, 713C, and 738X, were oxidized at 1000° and 1100° C in still air. The exposures were isothermal for 100 hours or for 100 one-hour heating cycles. The oxidation behavior was evaluated by specific weight change, sample thickness change, tendency for oxide spalling in the cyclic tests, X-ray diffraction of the retained and spalled scale(s), and metallography of selected test sample(s). At 1000° C, in both isothermal and cyclic testing the oxidation resistance was considered excellent to good for all four alloys although 738X spalled lightly in the cyclic exposures. At 1100° C, VIA and B-1900 still had excellent oxidation resistance in both isothermal and cyclic testing. Alloy 713C still showed excellent isothermal resistance, but with cycling the attack was about doubled. Although 738X had fair isothermal resistance, it spalled severely in cyclic exposures. The best oxidation resistance in this class of alloys is associated with αAl_2O_3/aluminate spinel formation based on approximately 6 weight percent aluminum and under 10 weight percent chromium present in the alloy. The poorer overall oxidation resistance is associated with Cr_2O_3/chromite spinel formation and its tendency to spall when termally cycled. Although the total refractory metal content of the alloy leads to tapiolite formation in the scale, it does not appear to affect the oxidation resistance.

INTRODUCTION

There has been an increased demand for higher strength nickel (Ni)-base alloys for use in gas turbine engines at temperatures approaching 1100° C. Increases in strength has been achieved largely by chemistry changes. These changes are in the direction of reducing chromium (Cr) content with accompanying increases in aluminum (Al) and titanium (Ti) to promote $Ni_3(Al, Ti)$ (or γ') strengthening. In addition, the refractory metal

content has been increased to improve solid solution (γ) strengthening. The increased strength has not necessarily been associated with improvements in oxidation resistance, however, and alloys have been coated, notably with NiAl (β).

The oxidation problem in nickel-base superalloys for aircraft engine use presents many uncertainties due both to the complexity of the oxidation process and to the difficulty of test design to simulate a gas turbine. The conventional isothermal test bears little relation to the turbine. A cyclic test, or even better, a cyclic test with high gas velocity comes closer. The question of the relation among the various tests is important for the progressive evaluation and development of alloys in a logical, meaningful, and economic manner.

Several good oxidation surveys have been made in recent years (refs. 1 and 2); however, they relate primarily to isothermal testing. A few isothermal studies have been made of specific superalloys (e.g., refs. 3 to 5), but again few cyclic data are available. An important exception is the work of Wasielewski (ref. 6). Such studies have found the oxidation of superalloys to be heterogeneous with many complex oxides being formed. This makes mechanistic evaluation difficult. One generalization has emerged; the closer to 100 percent Al_2O_3 the scale becomes, the greater the resistance of the alloy to oxidation. Alloys with high chromium contents favoring Cr_2O_3 formation are thought to be limited by Cr_2O_3 volatility above 1000° C (ref. 1).

This report is concerned with isothermal and cyclic furnace behavior of four selected nickel-base $\gamma + \gamma'$ alloys. They were furnace tested at 1000° and 1100° C in still air for 100 hours. Each cycle consisted of 1 hour at temperature and at least 40 minutes of cooling to allow the sample to reach near ambient temperature between cycles. These conditions were chosen as a compromise between use conditions and the desire to obtain sufficient oxidation in a reasonable time span to allow meaningful alloy comparison. Oxidation behavior was evaluated by and comparisons were made on the basis of specific sample weight change, X-ray diffraction, and metal recession. The latter involves metallographic evaluation of sample thickness change and depletion zone formation.

The four alloys chosen were the cast alloys NASA-TRW VIA, B-1900, 713C, and 738X. These all have $\gamma + \gamma'$ microstructures but cover a range of compositions. Table I lists the estimated 100-hour 1050° C rupture strengths and the nominal composition of these alloys in those elements expected to strongly enter into the oxidation process. Appreciable differences in chromium (5.9 to 15.8 percent), aluminum (3.6 to 6.2 percent), titanium (0.9 to 3.5 percent), and refractory metal content (6.3 to 17.9 percent) are apparent. (Refractory metals are defined as molybdenum, tungsten, rhenium, tantalum, and niobium. No distinction is made among the five although as pure metals molybdenum, tungsten, and rhenium tend to form volatile oxide scales at elevated temperatures. Tantalum and niobium form porous oxides which tend to crack and spall during isothermal exposures.)

In order to explain the relations between isothermal and cyclic furnace and high velocity oxidation tests, the four alloys were subjected to the three types of exposures. The major objectives were to define the oxidation processes of the several nickel-base superalloys, to rank the alloys, and to relate the oxidation processes to alloy chemistry. A secondary goal was to understand the relations of the various tests to one another as to mode and severity of oxidation.

This report is the second in a series of reports on cyclic superalloy oxidation. The first report deals with the high temperature X-ray diffraction of in situ oxides (ref. 7). A subsequent report will deal with high velocity oxidation.

EXPERIMENTAL PROCEDURES

The alloys were cast into bars approximately 10 by 2.5 by 0.64 centimeter. The chemical analysis of these alloys is shown in table II. All values fall within the standard specifications for these alloys. The microstructures of the four cast alloys are shown in figure 1.

After casting the alloys were given the following conventional heat treatments in argon for aircraft gas turbine applications:

VIA, 32 hours at 900° C, air cooled
B-1900, 4 hours at 1080° C, air cooled
713C, no treatment
738X, 2 hours at 1120° C, air cooled

The samples were next cut into 2.5 by 2.5 by 0.64 centimeter test specimens and then ground on all sides to remove approximately 0.025 centimeter. A hole was drilled as shown in figure 2, and all surfaces were glass bead blasted. Several thickness measurements were made along the line shown in figure 2 with a bench micrometer to a precision of ±1 micrometer. After these measurements, the samples were cleaned ultrasonically in tricholorethylene.

Isothermal oxidation was carried out at 1000° and 1100° C in still air for 100 hours. The apparatus used is shown in figure 3(a). A continuous recording electrobalance was used for measuring the weight change with a precision of ±0.1 milligram. The specimens were suspended by a thin quartz rod into the hot zone and by a platinum wire above the hot zone to the balance. The temperature was monitored and found to be constant within ±2° C. Cyclic oxidation was carried out in multitube automatic cyclic furnaces at 1000° and 1100° C for 100 hours. The apparatus used is shown in figure 3(b). Each cycle consisted of 1 hour in the hot zone followed by a minimum of 40 minutes out of the furnace. This 40-minute still air cooling cycle is arbitrary but allows the sample to be near room temperature for nearly 30 minutes.

The samples were automatically cycled in and out of the furnace by a pneumatic cylinder controlled by timers operating solenoid valves. The apparatus was equipped with a spall collector that was automatically positioned under the sample during the cooling portion of each cycle. Thus, spalls could be collected and analyzed. The specimens were weighed after 8, 24, 48, 72, and 100 cycles.

After testing, the samples were submitted for X-ray diffraction analysis; sufficient oxide for analysis was removed with a diamond abrasion tool. In addition, the spalls were analyzed. The samples were then mounted in epoxy and cut along the line of the original thickness measurements. After polishing, unaffected metal and alloy depletion were measured at several intervals using a traveling microscope with a maximum precision of ± 1 micrometer.

The thickness change determinations or recession values, which are based on the difference between the initial and final measurements, are discussed in detail in the appendix.

RESULTS AND DISCUSSION

Isothermal Oxidation

The alloy samples tested in isothermal oxidation were evaluated by four techniques: specific weight change, thickness change, X-ray diffraction, and metallography. The results are discussed in terms of these evaluation methods.

Specific weight change. - The average specific weight change results after several time intervals at 1000° and 1100° C are listed in table III. These values also appear in figure 4. At 1000° C (fig. 4(a)) there is very little difference between the curves of VIA, B-1900, and 713C. In comparison, 738X has a larger specific weight gain of 1.81 milligrams per square centimeter which after 100 hours at temperature is about four times greater than that of the three other alloys. At 1100° C (fig. 4(b)) there is a larger spread between the curves. Here B-1900 and 713C gained the least followed by VIA. Again 738X gained much more than the other alloys - close to 4.0 milligrams per square centimeter or about nine times as much as B-1900 after 100 hours at temperature. No attempt was made to determine oxidation mechanism or to compare the data with the usual rate laws. In such complex alloys the mode of oxidation in continuously changing and does not readily lend itself to the usual mechanistic type of analysis.

Thickness change. - The thickness change data are listed in detail in the appendix along with the associated error in the measurement(s). It can be generalized that for all the specimens tested isothermally at both temperatures the total metal thickness change values are effectively nonsignificant (see appendix). Thus, the total recession values are all nondistinguishable from the thickness of the depletion zone within experimental error.

At 1000^{o} C, after 100 hours, the depletion zones for VIA, B-1900, and 713C are all below 30 micrometers. The thickness of the depletion zone in 738X is well above this - 60 micrometers. At 1100^{o} C, after 100 hours. VIA and B-1900 have depletion zone thicknesses below 30 micrometers, 713C at 45 micrometers is just slightly higher, and the value for 738X is by far the largest at 120 micrometers.

X-ray diffraction analysis. - Tables IV(a) and (b) list the phases in the retained scale on the four alloys after the 8- and the 100-hour exposures. The phases detected in the spall are also listed whenever sufficient spall could be collected after a test for a determination. The spall is included as an indication of the total scale present during the test. The phases are listed in decreasing order of the intensity of their diffraction lines (i.e., the phase with the most intense peaks is listed first). In all cases the nickel alloy solid solution phase was detected in the analysis of the retained scale indicating that the X-rays penetrated to the base alloy.

At 1000^{o} C either αAl_2O_3 or tapiolite (Ni (Cb, Ta, Mo, W)$_2$ O_6-tetragonal structure) was the oxide phase with the most intensive diffraction lines on all the alloys except 738X. In this alloy Cr_2O_3 was the most prominent oxide detected. The spinels present both on B-1900 and particularly VIA were thought to be aluminates because of the low a_o values. The higher a_o value from the 100-hour B-1900 test still appeared to be an aluminate but with chromium replacing some of the aluminum. No spall was detected at this temperature.

At 1100^{o} C tapiolite remained the oxide phase with the most prominent lines on VIA. The 8-and 100-hour VIA specimen spalled. The 100-hour B-1900 specimen also spalled at 1100^{o} C. Here, in addition to tapiolite and αAl_2O_3, a spinel with an 8.25 Å lattice parameter was detected. This value is closer to a chromite (8.32 Å) than an aluminate (8.05 Å). For 713C, Cr_2O_3 was observed on the specimen exposed for 8 hours. This oxide was not seen on 713C for specimens exposed to any of the other test conditions. After 100 hours at 1100^{o} C, 713C spalled, and this is associated mainly with the presence of a chromite spinel and NiO. The oxide phases on 738X after 8 hours were the same at both temperatures. At 1100^{o} C the 100-hour specimen spalled. Both the retained scale and the spall contained a spinel, probably a chromite, in addition to Cr_2O_3 and tapiolite. The spall also contained NiO.

Metallography. - Figures 5 and 6 are cross sections of alloys exposed for 100 hours at 1000^{o} and 1100^{o} C. Essentially, the morphological difference between specimens exposed at the two temperatures is as expected (i. e., the γ' depletion zones are thicker in the respective specimen exposed at the higher temperature).

Summary of isothermal results. - Overall, B-1900 is probably the most oxidation resistant alloy although its behavior closely resembles VIA and 713C at both temperatures. By comparison, 738X is much less oxidation resistant. Good oxidation resistance is associated with the formation of αAl_2O_3 in the scale, and less resistance is associated with the presence of Cr_2O_3 and perhaps the chromite spinel. In those spec-

imens which spalled after exposure, either spinel and/or Cr_2O_3 was present along with the usual tapiolite in most cases. The role of the tapiolite in the overall isothermal oxidation process is not known.

Cyclic Oxidation

The alloy samples tested in cyclic oxidation were evaluated by the four techniques described in the isothermal oxidation section. An additional criterion used was an estimate of the amount of alloy spall after selected exposure cycles.

Weight change. - The specific sample weights for each alloy were determined at 1000° and 1100° C at 8, 24, 48, 72, and 100 hours. The spall was also collected, weighed, and examined at these intervals. The average specific spall weight for the number of samples tested is listed in table V after 8 and 100 cycles. This is the most immediate indication of the cyclic oxidation resistance of a given alloy. Because of some loss in collection, the spall weight is probably at best about 80 percent of the total. Obviously, just based on this relative indicator alone all four alloys have excellent spall resistance out to 100 hours at 1000° C. At 1100° C, VIA, B-1900, and 713C have good spall resistance while 738X appears to have much poorer spall resistance.

Conventional accumulated weight change curves ($\Delta w/A$ as function of time) were also plotted for each alloy based on the average $\Delta w/A$ values at 8, 24, 48, 72, and 100 hours. These average values and the overall standard deviation for each alloy at each temperature are listed in table VI and the average $\Delta w/A$ values are plotted in figures 6(a) and (b) for 1000° and 1100° C, respectively. At 1000° C, the three lower curves resemble the isothermal curves showing that spalling is negligible. This agrees with the negligible amount of spall collected at 1000° C. Alloy 738X had a much higher scaling rate, however, since its total weight gain at 100 hours of 2.61 milligrams per square centimeter was at least five times higher than the other three alloys. At 1100° C all four alloys show increasingly negative values with time implying oxide spalling (and possibly vaporization). The four alloys can be classified in three distince groupings, however. Alloys VIA and B-1900 have almost identical $\Delta w/A$ against time curves out to 100 hours. They are just barely negative (-0.68 and -0.60 mg/cm^2, respectively), and this coupled with the moderate amount of spall collected indicates good cyclic oxidation resistance. Alloy 713C shows an increasingly severe weight loss close to 5 milligrams per square centimeter at 100 hours, which is almost eight times that of VIA and B-1900. Alloy 738X is much more severe with the 100-hour weight loss some 40 times that of VIA and B-1900. In general, the amount of spall tends to complement these specific weight loss values although the spall weight of 1.35 milligrams per square centimeter (table V) was somewhat lower than expected for the 713C weight loss at 100 hours.

Thickness change. - The thickness change was measured metallographically for each

alloy at each test interval along with any depletion zone for γ' as described previously. The complete values are listed in the appendix along with the associated experimental error estimates. Both the total metal thickness change and surface depletion zone are used as a combined parameter termed total recession to rate the severity of oxidation. This parameter should be equally valid for both cyclic and isothermal oxidation as opposed to the specific weight change. At 1000° C, however, the total metal thickness change measured is not distinguishable from the experimental error. The 1000° C depletion values are significant, but they show no time trend for VIA, B-1900, and 713C. They are all less than 30 micrometers at all times. Alloy 738X at 1000° C did show an increased depletion zone attack with time, up to three times the depletion zone values of the other three alloys. The total recession values up to 80 micrometers after 100 cycles are probably the most meaningful for 738X because, except for the 8-hour value, they all exceed the measurement error by at least 2 sigma.

At 1100° C, the trends are more obvious due to increased severity of attack. Alloys VIA and B-1900 seem to be about the same in total recession again as at 1000° C (less than 30 μm total consumption after 100 hr). Alloy 713-C appears to have at least twice and 738X roughly 10 times the total oxidation attack of alloys VIA and B-1900. The 100-cycle total recession values are 89 and 322 micrometers, respectively, for 713C and 738X. Alloys 738X and to some extent 713C show the expected severe attack with time, as well, in line with the specific weight change data and the amount of spall observed.

X-ray diffraction analysis. - To attempt to interpret the cyclic oxidation process, X-ray diffraction analyses (XRD) were performed on both the spalled and the retained oxides. In cyclic tests the nature of the spall is critical to the complete oxidation process. The analyses were run for each alloy oxidized at 1000° and 1100° C at intervals of 0 to 8 and 72 to 100 cycles. These results are summarized in table VII.

At 1000° C both VIA and B-1900 show generally similar results. The γ (or γ') solid solution line is visible to the X-ray beam, which indicates scraping included the metal substrate. The observed spinel is thought to be mainly $NiAl_2O_4$ although the a_o values of 8.20 Å are somewhat high, indicating some chromium replaces the aluminum. It appears this spinel confers the alloys' good oxidation resistance. Tapiolite ($Ni(Cb, Ta, Mo, W)_2O_6$) is also detected. There was no detectable spall. Alloy 713C shows slightly different behavior at 1000° C. At a later time αAl_2O_3 was detected instead of the 8.20 Å spinel, but the alloy had about the same oxidation resistance as VIA and B-1900. Alloy 738X appears to be mainly a Cr_2O_3 former at 1000° C, and this apparently accounts for its greater scaling rate shown in the $\Delta w/A$ against time plot (in fig. 6). Again tapiolite is detected. The slight spalling of this alloy is probably due to the thicker oxide formed.

The 1100° C cyclic oxidation behavior seems, in general, to be more complex. The VIA and B-1900 alloys oxidize similarly, and in some respects their 1100° C behavior resembles their 1000° C behavior. In addition, NiO and Cr_2O_3 are found here. These two alloys show light to moderate spalling at 1100° C. It is not evident what causes this

spalling. Alloy 713C now forms an 8.10 Å spinel instead of the αAl_2O_3, but the spalling is probably associated with NiO and a higher a_o spinel (8.25 Å) being formed. The severe spalling found with 738X is believed associated with Cr_2O_3/chromite spinel formation. It is not clear when the more protective, less spall prone aluminate spinel becomes the less protective, more spall prone chromite spinel. This transition appears to occur around an a_o value of 8.25 Å. It also seems associated with the scale becoming a more intense blue in color.

Tapiolite is omnipresent in nearly all the sample's oxides. It is thought that its role in spalling is not significant.

Metallography. - Figure 7 shows the metal/oxide interface including the γ' depletion zone (on the right) and the $\gamma + \gamma'$ metal substrate for each of the four alloys after 100 cycles at 1000° and 1100° C. The nearly regular depletion zones are the most striking feature noted in the figures due to the conversion of mainly aluminum (VIA, B-1900, and 713C) or chromium (738X) to oxide scale. This depletion results from the conversion of γ' to γ and is considered part of the overall oxidation attack as well, since the high temperature, high strength phase γ' is uniformly diminished in the depletion zone. Another feature is the internal oxidation or oxide penetration present in the 738X alloy at 1000° C within the depletion zone.

Summary of cyclic results. - A comparison by the four evaluation techniques of the cyclic data at 1000° and 1100° C shows both VIA and B-1900 have good cyclic oxidation resistance and do not differ significantly at the two test temperatures. Alloy 713-C behaves similarly to VIA and B-1900 at 1000° C, but it shows a significant increase in oxidation attack at 1100° C in terms of specific weight loss and has a total recession of about twice that at 1000° C. Alloy 738X shows at least twice the attack at 1000° C of the other three alloys based on both total recession and on specific weight change. At 1100° C, total recession values, specific weight loss, and total spall indicated that for 738X total oxidation attack is about four times that at 1000° C or eight times that of the other alloys at 1100° C. The increased oxidation and spalling tendency is associated with Cr_2O_3/chromite spinel formation.

Comparison of Isothermal and Cyclic Oxidation

The four techniques used to evaluate and interpret the oxidation behavior of the alloys - specific weight change, thickness change, X-ray diffraction, and metallography - were also used to compare the isothermal and cyclic oxidation resistance. These data are summarized in table VIII for the four alloys after 100 hours of oxidation at both temperatures. At 1000° C and after 100 hours, except for 738X, the spalling was negligible in the cyclic tests. On this basis, the $\Delta w/A$ against time curves, thickness changes,

X-ray diffraction results, and metallography should be very similar for both tests. This is indeed true as a comparison of the results in table VIII shows for VIA, B-1900, and 713C. The $\Delta w/A$ values and overall recession agree to within about 20 percent - the usual run to run variation in a cyclic test in these rigs. For these basically αAl_2O_3/ aluminate spinel forming alloys, the XRD and metallography are similar as well. In cyclic testing, on the other hand, 738X at 1000° C appears to oxidize at about one and one-half times the rate as the isothermally tested 738X. Even though the spalling rate for 738X can be considered low, in as early as 8 hours the cyclic oxygen pickup is considerably higher than that of the comparable isothermal test. Although this weight change difference between the two types of tests is apparently real since several samples were involved, it is not understood.

At 1100° C, compared to the isothermally tested samples, the cyclic oxidation resistance is reduced due to spalling. This comparison is shown in figure 8 in terms of specific weight change with time and in table VIII for the 100-hour results. For VIA and B-1900 this is not as obvious from thickness data and metallography as it is from weight change results and from the moderate amounts of spall collected throughout the test. For practical purposes, however, from the standpoint of depletion and recession, the 100-hour isothermal and cyclic (1-hr heating cycles) oxidation behavior of VIA and B-1900 at 1100° C can be considered to be about the same.

For 713C and 738X, the weight change data alone would indicate spalling in cyclic oxidation significantly increases the overall oxidation rate compared to the isothermal tests. The recession results indicate this increase is about a factor of 2 or 3. For 713C this increase is apparently due to the NiO, Cr_2O_3, and chromite spinels being formed in addition to the thinner less spall prone Al_2O_3/aluminate spinels, resulting in a thicker scale for cyclically tested material. For 738X, Cr_2O_3 is controlling oxidation. This oxide becomes more spall prone as it gets thicker and as NiO is also formed leading to chromite spinel formation.

Comparison of Alloy Chemistries and Oxidation Processes

The oxidation behavior of these alloys can be viewed as follows: Alloys VIA and B-1900 at 1000° and 1100° C appear to have high enough aluminum content (>5 percent) and minimal chromium (<10 percent) content so that the αAl_2O_3/aluminate spinel can form and control the rate of scale buildup. The scale stays thin enough (though slightly thicker at 1100° C) out to 100 hours so that spalling is slight when cycled. Alloy 713C behaves like alloys VIA and B-1900 up to a point, particularly at 1000° C, but its higher chromium content (~12 percent) allows Cr_2O_3, NiO, and the chromium rich spinel to eventually form, which leads to spalling when cycled at 1100° C. Alloy 738X because of its higher chromium content (16 percent) and lower aluminum content (~3.5 percent)

is basically a Cr_2O_3/chromite spinel former at both 1000° and 1100° C. This leads to a thicker more spall prone oxide (especially at 1100° C) than found on the αAl_2O_3/aluminate spinel formers. The role of aluminum in the oxidation of 738X appears minimal. The refractory metals apparently lead only to the formation of tapiolite on all the alloys, but this oxide does not seem to affect the oxidation behavior. The fact that the two alloys with the best oxidation resistance of the four tested have the highest total refractory metal content indicates that refractory metal additions are not particularly harmful up to at least the 18 percent level. This makes no distinction between the types of refractory metal, however. Neither titanium nor rhenium were apparent in any of the oxides. Their role(s) in the oxidation processes is unknown.

SUMMARY OF RESULTS

Four selected nickel-base cast $\gamma + \gamma'$ alloys with a range of chromium, aluminum, and refractory metal contents (NASA-TRW VIA, B-1900, 713, and 738X) were exposed isothermally for up to 100 hours or for up to 100 one-hour cycles in still air at 1000° and 1100° C. The oxidation behavior of the samples was evaluated by specific weight change, measured surface recession, X-ray diffraction, and metallography. Measured total recession is a combination of metal loss and depletion zone formation. The amount of spall collected during the cyclic tests was also used as an indicator of cyclic oxidation behavior. The results can be summarized as follows:

1. The alloys with the lowest chromium content (6 to 8 percent) and close to 6 percent aluminum (VIA and B-1900) had the best overall oxidation resistance (both isothermal and cyclic) at 1000° and 1100° C. The thin protective scale formed was mainly αAl_2O_3/aluminate spinel.

2. Alloy 713C with ~6 percent aluminum behaved like alloys VIA and B-1900 at 1000° C, but at 1100° C its higher chromium content (close to 14 percent) allowed both Cr_2O_3 and NiO and their spinel to form.

3. Alloy 738X with 16 percent chromium and 3.5 percent aluminum was basically a Cr_2O_3/chromite spinel forming alloy which formed a much thicker scale than the other three alloys. The chromite spinel lead to spalling on thermal cycling.

4. All the alloys showed the presence of tapiolite - $Ni(Cb, Ta, Mo, W)_2 O_6$ - in the scales in nearly all oxidation conditions. This oxide was formed from the refractory metals present in the alloys, the amount of which ranged from 6 (713C) to 18 (VIA) percent. Refractory metal content appears to have no significant effect on the oxidation behavior of any of the four alloys tested, however. The role of titanium in the total oxidation process was not apparent.

5. At 1000° C the isothermal and cyclic oxidation behavior of the αAl_2O_3/aluminate spinel forming alloys (VIA, B-1900, and 713C) were similar and showed low specific

weight gain (<1.0 mg/cm^2) and low total recession values (<30 μm) after 100 hours. Spalling was negligible for the samples run in the cyclic tests. For the Cr_2O_3/chromite spinel forming alloy (738X) the oxygen pickup was about 2.0 milligrams per square centimeter and total recession was 60 micrometers after 100 hours. The cyclic sample showed slight spalling and a total recession of 80 micrometers.

6. At 1100^o C, the isothermal behavior of the αAl_2O_3/aluminate spinel forming alloys (VIA, B-1900 and 713C) resembled that at 1000^o C with an upper specific weight change value of 1.5 milligrams per square centimeter being observed along with total recessions of less than 50 micrometers. When cycled the alloys showed moderate spalling along with negative specific weight change values. Alloy 713C showed enough Cr_2O_3 present to form a chromite spinel associated with thicker scales and increased spalling. For alloys VIA and B-1900, the cyclic total recession values were similar to the isothermal values. For alloy 713C, the cyclic total recession value was close to 90 micrometers. For the straight Cr_2O_3/chromite spinel forming alloy 738X tested isothermally, the oxygen pickup and total recession were about double the 1000^o C values. When cyclic testing alloy 738X, the spalling was heavy, which reflected a specific weight loss of nearly 28 milligrams per square centimeter and a total recession of over 300 micrometers.

CONCLUDING REMARKS

Based on this study both NASA-TRW VIA and B-1900 form the αAl_2O_3/aluminate spinel scale needed to confer good oxidation resistance even in cyclic oxidation out to 100 hours at 1100^o C. Longer time tests, possibly with more severe cycling (e.g., 0.1 hr cycles), would be required to definitely establish the more resistant alloy. The long time effect of tapiolite on the cyclic oxidation could be critical as well.

It is not known what the optimum chromium and aluminum contents or Al/Cr ratio should be to maintain αAl_2O_3/aluminate spinel formation control as long as possible in $\gamma + \gamma'$ alloys before a critical amount of spall prone chromite spinel forms. The interaction of these chromium and aluminum contents with total or individual refractory metal content(s) could also be important. Also, the role of titanium in the oxidation process was not defined in this study. Volatile oxides like MoO_3 might form in preference to tapiolite if the molybdenum, rhenium, and/or tungsten contents are too high. An optimal seeking technique based on aluminum, chromium, and refractory metal content similar to that used developing other γ' strengthened alloys (ref. 8) might be useful to maximize temperature oxidation resistance of such alloys. A combined strength and cyclic oxidation resistance might be optimized using a Box-Wilson approach (ref. 9, pp. 495 to 498). Lowering the chromium content well under 10 percent may lower the resistance to hot corrosion at lower temperatures, however.

The advantages of cyclic oxidation furnace testing as an evaluation tool for gas turbine alloys is apparent vis-a-vis isothermal testing. For alloys that are αAl_2O_3/aluminate spinel formers, the oxidation behavior in cyclic tests should resemble that in a high velocity burner rig since negligible scale vaporization is expected.

Lewis Research Center,
National Aeronautics and Space Administration,
Cleveland, Ohio, August 22, 1973,
501-01.

APPENDIX - DETERMINATION AND VARIABILITY OF THICKNESS CHANGE MEASUREMENTS

The type of thickness measurements made before and after testing are shown schematically in the following sketch. The initial measurement t_o is made with a bench

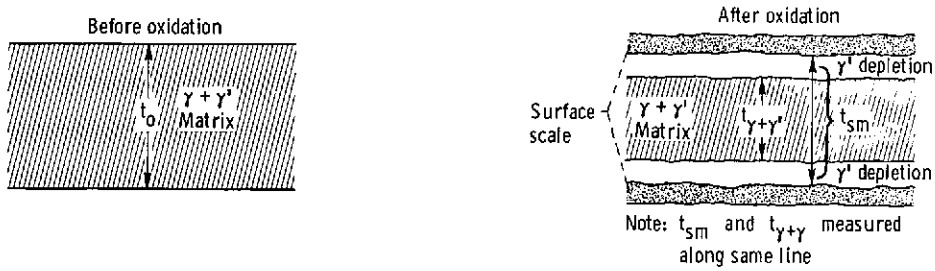

micrometer to the nearest micrometer at five locations as was indicated in figure 2 across the center of the sample. These five values are averaged to give a mean initial thickness $\bar{t}_o$. After testing the samples are mounted in epoxy and sectioned perpendicularly across the center, polished, and then etched. The total thicknesses between the oxide scales are determined (also to the nearest micrometer) this time by a traveling microscope at the same estimated five pretest locations. These t_{sm} values are then averaged for a mean value $\bar{t}_{sm}$. At each location for each t_{sm} measurement the γ' depletion zone is also measured by measuring the $\gamma + \gamma'$ layer termed $t_{\gamma+\gamma'}$ and then subtracting it from its corresponding t_{sm} to give t_d (the total thickness of the depletion zone). These five t_d values are averaged for a mean value $\bar{t}_d$. All of these sample measurements have a certain error or variability associated with them. For the initial measurement $\bar{t}_o$, it is due to variation in thickness across the sample. Only a gage block would be expected to have no significant variation when measured to the nearest micrometer. Twelve random specimens, each with five t_o estimates, were used for each alloy to determine individual specimen variances. These were then pooled to determine the variance associated for the $\bar{t}_o$ estimates for each alloy (ref. 9, pp. 285 to 289). The square root of this alloy variance is the standard deviation associated with each specimen $\bar{t}_o$. These are listed in table IX. Even though all the alloys were apparently cast and prepared in the same manner, the 713C alloy samples had significantly greater thickness variability than the other three alloys.

The samples after oxidation probably still have thickness variations under the scale as a function of the original thickness variability before oxidation as well as any contribution due to scale formation. This variation was determined for all the t_{sm} values for each alloy by again calculating each sample variance for the five measurements. For

each alloy these individual sample variances appeared homogeneous and were pooled as before. These values are listed in table IX for both the isothermal and cyclic tested alloys. Since the overall total metal thickness changes,

$$\Delta\bar{t}_{sm-0} = \bar{t}_o - \bar{t}_{sm}$$

the variance of the measurement for each alloy is the sum of the t_o and t_{sm} variances. The square root of this summed variance is the standard deviation σ_{sm-0} of the total metal thickness change measurement. These are also listed in table IX for each alloy.

The depletion zone variance for each alloy under cyclic or isothermal conditions was derived from the pooled specimen variances calculated from the five $(t_{sm} - t_{\gamma+\gamma'})$ values for each sample. The only nonhomogeneous variances were the 738X 1100° C cyclic 72- and 100-hour samples which had much larger depletion zone variances associated with the large total metal thickness change. These standard deviations are also listed in table IX.

The total recession is defined as

$$\Delta\bar{t}_{total} = \Delta\bar{t}_{sm-0} + \bar{t}_d$$

Therefore,

$$\sigma^2_{total} = \sigma^2_{sm} + \sigma^2_{t_o} + \sigma^2_d$$

This summation is used only for specimens for which the $\Delta\bar{t}_{sm-0}$ value is considered significant (i.e., when this value is effectively nonzero). When $\Delta\bar{t}_{sm-0}$ is not significant, the $\Delta\bar{t}_{total}$ is not distinguishable from $\bar{t}_d$. All the average thickness changes for the isothermal and cyclic tests for each alloy are listed in table X for all the alloys at each temperature. The $\Delta\bar{t}_{sm-0}$ values are designated as nonsignificant in table X when they fall within $\pm 1\frac{1}{2}$ standard deviation units of zero.

REFERENCES

1. Wright, I. G.: Oxidation of Iron-, Nickel-, and Cobalt-Base alloys. Rep. MCIC-72-07, Metals and Ceramics Information Center, Batelle Memorial Inst. (AD-745473), June 1972.

2. Rentz, W. A.; and Donachie, M. J., Jr.: Oxidation and Sulfidation Corrosion of Nickel Base Superalloys. Tech. Rep. No. C6-18.5, ASM, Oct. 1966.

3. Rosenberg, Robert A.: Oxidation of Rene 41 and Thoriated Nickel Wires Between 1600° and 2000° F. Mach/GAW-18-64, Air Force Inst., Tech. (AD-610241), June 1964.

4. Baciarelli, R. M.: Army Gas-Cooled Reactor Systems Program. Isothermal Oxidation of Hastelloy X at 1750° and 1850° F in Air. Rep. AGN TM-413, Aerojet-General Nucleonics, Dec. 1965.

5. Waters, W. J.; and Freche, J. C.: A High Strength Nickel-Base Alloy with Improved Oxidation Resistance up to 2200° F. J. Eng. Power, vol. 90, no. 1, Jan. 1968, pp. 1-10.

6. Wasielewski, G. E.: Nickel-Base Superalloy Oxidation. General Electric Co. (AFML-TR-67-30, AD-809831), Jan. 1967.

7. Garlick, Ralph G.; and Lowell, Carl E.: Alloy Composition Effects on Oxidation Products of VIA, B-1900, 713C, and 738X - a High Temperature Diffractometer Study. NASA TM X-2796, 1973.

8. Sandrock, Gary D.; and Holms, Arthur G.: Statistical Design and Analysis of Optimum Seeking Experiments to Develop a Gamma-Prime Strengthened Cobalt-Nickel Base Alloy. NASA TN D-5587, 1969.

9. Davies, Owen L., ed.: The Design and Analysis of Industrial Experiments. Hafner Publ. Co., 1956.

TABLE I. - KEY ELEMENT CONTENT AND STRESS RUPTURE LIFE FOR FOUR NICKEL-BASE ALLOYS

[All composition values are in weight percent. |

Alloy	Stress for 100-hr rupture life at 1050° C, N/m^2	Chromium	Aluminum	Titanium	Refractory metals		
					Total	Molybdenum, tungsten, rhenium (a)	Tantalum, niobium (b)
VIA	144×10^6	5.9	5.3	1	17.9	8.4	9.5
B-1900	103	8.0	6.2	1.1	10.3	6.1	4.2
713C	90	13.6	6.0	.9	6.3	4.2	2.1
738X	96	15.8	3.6	3.6	7.0	4.5	2.5

3[a]As pure metal forms, volatile oxide(s) at elevated temperatures.
3[b]As pure metal forms, porous oxide(s) at elevated temperatures.

TABLE II. - CHEMICAL ANALYSIS OF CAST ALLOYS IN WEIGHT PERCENT.

Element	Alloy			
	VIA	B-1900	713C	IN-738X
	Chemical analysis, wt%			
Chromium	5.86	7.99	13.64	15.84
Cobalt	7.24	10.00	.53	8.81
Aluminum	5.27	6.18	6.00	3.57
Titanium	.95	1.11	.87	3.39
Boron	.021	.014	.009	.01
Zirconium	.10	.06	.10	.08
Carbon	.11	.12	.13	.16
Tantalum	9.03	4.14	(a)	1.68
Niobium	.45	<.05	(a)	.85
Molybdenum	2.11	6.05	4.18	1.70
Tungsten	5.96	<.05	NA[b]	2.78
Iron	.08	<.10	.39	<.10
Rhenium	.32	NA	NA	NA
Hafnium	.39	NA	NA	NA
Copper	<.05	NA	<.10	<.08
Manganese	.02	<.02	<.05	<.02
Sulfur	.008	.007	.009	.006
Silicon	<.10	<.05	.17	<.50
Nickel	Remainder	Remainder	Remainder	Remainder

[a]Ta + Nb =2.10.
[b]Not analyzed.

TABLE III. - SPECIFIC WEIGHT CHANGE RESULTS FOR ISOTHERMAL SUPERALLOY OXIDATION IN STILL AIR

[Standard deviation, σ- replication error based on pooled variances at 8, 24, 48, and 72 hr.]

Alloy	Temperature, ^{o}C									
	1000					1100				
	Time[a], hr									
	8	24	48	72	100	8	24	48	72	100
	Average specific weight change results, mg/cm^2									
	$\sigma = \pm 0.02$					$\sigma = \pm 0.04$				
VIA	0.16	0.25	0.33	0.39	0.41	0.52	0.86	1.14	1.33	1.51
	$\sigma = \pm 0.08$					$\sigma = \pm 0.06$				
B-1900	0.12	0.19	0.28	0.32	0.45	0.19	0.25	0.32	0.34	0.49
	$\sigma = \pm 0.02$					$\sigma = \pm 0.12$				
713C	0.12	0.17	0.21	0.23	0.25	0.49	0.65	0.67	0.71	0.69
	$\sigma = \pm 0.14$					$\sigma = \pm 0.44$				
738X	0.26	0.50	0.86	1.19	1.81	0.92	1.77	2.59	3.25	4.01

[a]8 Hours, average of 5 runs; 24 hours, average of 4 runs; 48 hours, average of 3 runs; 72 hours, average of 2 runs; 100 hours, single run value.

TABLE IV - PHASES IDENTIFIED BY X-RAY DIFFRACTION AFTER ISOTHERMAL OXIDATION AT 1000° AND 1100° C IN STILL AIR

[Phases listed in decreasing order of pattern intensity but not necessarily related to quantity in sample. $NiAl_2O_4$ spinel, a_o = 8.05 Å; $NiCr_2O_4$ spinel, a_o = 8.32 Å; tapiolite, $NiCb(Ta, Mo, W)_2O_6$; nickel solid solution, γ and/or γ'.]

(a) Temperature, 1000° C.

Alloy	Time at temperature, hr	Oxide	
		Scraped	Spalled
VIA	8	Nickel solid solution Tapiolite αAl_2O_3 Spinel (a_o = 8.10 Å)	- - - -
	100	Nickel solid solution Tapiolite αAl_2O_3 Spinel (a_o = 8.10 Å)	- - - -
B-1900	8	Nickel solid solution αAl_2O_3 Cr_2O_3	- - - -
	100	Nickel solid solution αAl_2O_3 Tapiolite	- - - -
713C	8	Nickel solid solution αAl_2O_3 Tapiolite	- - - -
	100	Nickel solid solution αAl_2O_3 Tapiolite	- - - -
738X	8	Nickel solid solution Cr_2O_3 Tapiolite	- - - -
	100	Nickel solid solution Cr_2O_3 Tapiolite	- - - -

(b) Temperature, 1100° C.

Alloy	Time at temperature, hr	Oxide	
		Scraped	Spalled
VIA	8	Nickel solid solution Tapiolite αAl_2O_3 Spinel (a_o = 8.10 Å) Spinel (a_o = 8.30 Å)	- - - -
	100	Nickel solid solution Tapiolite Spinel (a_o = 8.10 Å) αAl_2O_3	Tapiolite Cr_2O_3
B-1900	8	Nickel solid solution αAl_2O_3 Tapiolite	- - - -
	100	Nickel solid solution αAl_2O_3 Tapiolite	αAl_2O_3 Nickel solid solution Spinel (a_o = 8.25 Å)
713C	8	Nickel solid solution Tapiolite αAl_2O_3 Cr_2O_3	- - - -
	100	Nickel solid solution αAl_2O_3 Tapiolite	Spinel (a_o = 8.25 Å) NiO αAl_2O_3
738X	8	Nickel solid solution Cr_2O_3 Tapiolite	- - - -
	100	Cr_2O_3 Spinel (a_o = 8.25 Å) Tapiolite Nickel solid solution	Cr_2O_3 Tapiolite NiO Spinel (a_o = 8.25 Å)

TABLE V. - COLLECTED ACCUMULATIVE SPECIFIC CYCLIC SPALL WEIGHT IN STILL AIR

[Estimated percent of actual spall collected, ~80 percent upper limit; 1-hr heating cycles.]

Alloy	Exposure temperature, ^{o}C			
	1000		1100	
	Time, hr			
	1 to 8	1 to 100	1 to 8	1 to 100
	Average specific spall weight, mg/cm^2			
VIA	~0	~0	0.01	1.27
B-1900	~0	~0	.08	.83
713C	~0	~0	.59	1.35
738X	~0	0.06	.23	21.00

TABLE VI. - AVERAGE VALUES OF ACCUMULATED WEIGHT CHANGE AND OVERALL STANDARD DEVIATIONS FOR EACH ALLOY IN STILL AIR AT 1000^{o} AND 1100^{o} C

[Type of oxidation, cyclic; 1-hr heating cycles; standard deviation, σ-replication error based on pooled variances at 8, 24, 48, 72, and 100 hr.]

Alloy	Temperature, ^{o}C									
	1000					1100				
	Time,[a] hr									
	8	24	48	72	100	8	24	48	72	100
	Average specific weight results, mg/cm^2									
	σ = ±0.06					σ = ±0.15				
VIA	0.35	0.38	0.42	[b]0.38	0.51	0.64	0.41	0.13	-0.19	-0.68
	σ = ±0.03					σ = ±0.07				
B-1900	0.14	0.17	0.21	0.27	0.27	0.34	0.03	-0.15	-0.36	-0.60
	σ = ±0.03					σ = ±0.48				
713C	0.14	0.28	0.31	0.29	0.32	-0.99	-1.26	-2.18	[c]-3.32	-4.71
	σ = ±0.10					σ = ±0.94				
738X	0.78	1.35	2.29	2.59	2.61	1.75	0.78	-12.27	-16.94	-27.56

[a]8 Hours, average of 6 values; 24 hours, average of 5 values; 48 hours, average of 4 values; 72 hours, average of 3 values; 100 hours, average of 2 values.

[b]74 Hours.

[c]73 Hours.

TABLE VII. - PHASES IDENTIFIED BY X-RAY DIFFRACTION AFTER CYCLIC OXIDATION (1-HR HEATING CYCLES) AT 1000° AND 1100° C IN STILL AIR

[Phases listed in decreasing order of intensity but not necessarily related to quantity in sample. $NiAl_2O_4$ spinel, a_o = 8.05 Å; $NiCr_2O_4$ spinel, a_o = 8.32 Å; tapiolite, $NiCb(Ta, Mo, W)_2O_6$; nickel solid solution, γ and/or γ'.]

(a) Temperature, 1000° C.

Alloy	Time at temperature, hr	Oxide	
		Scraped	Spalled
VIA	1 to 8	Nickel solid solution Tapiolite Spinel (8.20 Å) αAl_2O_3	- - - -
	72 to 1000	Nickel solid solution Tapiolite Spinel (8.20 Å)	- - - -
B-1900	1 to 8	Nickel solid solution Tapiolite NiO Spinel (8.20 Å)	- - - -
	72 to 100	Nickel solid solution Tapiolite Spinel (8.20 Å)	- - - -
713C	1 to 8	Nickel solid solution	- - - -
	72 to 100	Nickel solid solution Tapiolite αAl_2O_3	- - - -
738X	1 to 8	Nickel solid solution Cr_2O_3 Tapiolite	- - - -
	72 to 100	Cr_2O_3 Tapiolite Nickel solid solution	Cr_2O_3 Tapiolite

(b) Temperature, 1100° C.

Alloy	Time at temperature, hr	Oxide	
		Scraped	Spalled
VIA	1 to 8	Nickel solid solution Tapiolite Spinel (8.20 Å) NiO	Tapiolite Spinel (8.20 Å) Cr_2O_3
	72 to 100	Nickel solid solution Tapiolite Spinel (8.15 Å) NiO	Tapiolite Spinel (8.15 Å)
B-1900	1 to 8	Nickel solid solution Tapiolite Spinel (8.15 Å) Cr_2O_3 NiO	NiO Tapiolite Spinel (8.20 Å) Cr_2O_3
	72 to 100	Nickel solid solution Tapiolite Spinel (8.15 Å) NiO αAl_2O_3	NiO Tapiolite Spinel (8.20 Å) Nickel solid solution
713C	1 to 8	Nickel solid solution NiO Tapiolite Spinel (8.10 Å)	NiO Spinel (8.25 Å) Cr_2O_3
	72 to 100	Nickel solid solution Spinel (8.10 Å) Tapiolite	Nickel solid solution Spinel (8.25 Å) Tapiolite
738X	1 to 8	Cr_2O_3 Tapiolite Nickel solid solution	Cr_2O_3 Tapiolite Nickel solid solution NiO
	72 to 100	Nickel solid solution NiO Tapiolite Spinel (8.30 Å) Cr_2O_3	Tapiolite Nickel solid solution Spinel (8.25 Å) Cr_2O_3

TABLE VIII. - SUMMARY OF OXIDATION RESULTS AFTER 100 HOURS IN STILL AIR AT 1000^{o} OR 1100^{o} C

[Mainly Al spinel, a_o = 8.05 to 8.20 Å; mainly Cr spinel, a_o = 8.25 to 8.32 Å; assume Al and Cr can substitute interchangeably in spinel.]

(a) Temperature, 1000^{o} C.

Alloy	Type of test	Specific weight change, mg/cm^2	Depletion (γ') zone, μm	Total recession, μm (a)	Oxide phases identified by x-ray diffraction
VIA	Isothermal	0.41	15	~15	Tapiolite αAl_2O_3 Al spinel
	Cyclic (collected spall)	.51 (0)	15	~15	Tapiolite αAl_2O_3 Al spinel
B-1900	Isothermal	0.45	13	~13	Tapiolite αAl_2O_3
	Cyclic (collected spall)	.27 (0)	9	~9	Tapiolite αAl_2O_3 Al spinel NiO
713C	Isothermal	0.25	16	~16	Tapiolite αAl_2O_3
	Cyclic (collected spall)	.32 (0)	14	~14	Tapiolite αAl_2O_3
738X	Isothermal	1.81	60	~60	Tapiolite Cr_2O_3
	Cyclic (collected spall)	2.61 (0.06)	55	80	Tapiolite Cr_2O_3

[a]Summation of depletion zone and total metal consumed; ~ indicates total metal consumed not significant (between $\pm 1.5\sigma$) and significant contribution due to depletion only.

(b) Temperature, 1100^{o} C.

Alloy	Type of test	Specific weight change, mg/cm^2	Depletion (γ') zone, μm	Total recession, μm (a)	Oxide phases identified by x-ray diffraction
VIA	Isothermal	1.51	28	~28	Tapiolite αAl_2O_3 Al spinel Cr_2O_3
	Cyclic (collected spall)	-.68 (1.27)	28	~28	Tapiolite Al spinel Cr_2O_3 NiO
B-1900	Isothermal	0.49	21	~21	Tapiolite αAl_2O_3 Al spinel
	Cyclic (collected spall)	-.60 (.83)	14	~14	Tapiolite αAl_2O_3 Al spinel Cr_2O_3 NiO
713C	Isothermal	0.69	45	~45	Tapiolite αAl_2O_3 Al spinel Cr_2O_3 NiO
	Cyclic (collected spall)	-4.71 (1.35)	61	89	Tapiolite αAl_2O_3 Al spinel Cr_2O_3 Cr spinel NiO
738X	Isothermal	4.01	120	~120	Tapiolite Cr_2O_3 Cr spinel NiO
	Cyclic (collected spall)	-27.56 (21.00)	222	322	Tapiolite Cr_2O_3 Cr spinel

TABLE IX. - STANDARD DEVIATIONS FOR VARIOUS THICKNESS MEASUREMENTS ON UNOXIDIZED AND OXIDIZED ALLOY SAMPLES

[Values, in μm, derived from square root of pooled sample variances.]

Alloy	Initial sample variability, σ_{t_o}	Posttest sigma values at 1000^{o} and 1100^{o} C			
		Between oxide scale, σ_{SM-O}		γ' Depletion zone, σ_d	
		Isothermal	Cyclic	Isothermal	Cyclic
VIA	6	15	24	3	3
B-1900	6	8	9	3	2
713C	14	22	19	4	6
738X	4	10	11	7	[a]5

[a] σ_d for 72 and 100 cycles at 1100^{o} C, 31.

TABLE X. - AVERAGE ALLOY RECESSION VALUES MEASURED AFTER ALLOY OXIDATION IN STILL AIR AT 1000° OR 1100° C

Alloy	Time at temperature, hr	Temperature, °C											
		1000						1100					
		Total metal thickness change, $\Delta\bar{t}_{SM-O}$		Formation of γ' depletion zone, $\bar{t}_d$		Total recession, $\Delta\bar{t}_{total}$		Total metal thickness change, $\Delta\bar{t}_{SM-O}$		Formation of γ' depletion zone, $\bar{t}_d$		Total recession, $\Delta\bar{t}_{total}$	
		I[a]	C[b]	I	C	I	C	I	C	I	C	I	C
		Alloy recession values, μm											
VIA	8	NS[c]	NS	NS	13	NS	13	NS	NS	19	23	19	23
	24	↓	↓	↓	8	↓	8	↓	↓	18	29	18	29
	48	↓	↓	↓	9	↓	9	↓	↓	21	29	21	29
	72	↓	↓	↓	16	↓	16	↓	↓	26	27	26	27
	100	↓	↓	15	15	15	15	↓	↓	28	28	28	28
B-1900	8	NS	NS	11	5	11	5	NS	NS	12	20	12	20
	24	↓	↓	10	4	10	4	↓	14	9	13	9	27
	48	↓	↓	12	8	12	8	↓	22	12	13	12	35
	72	↓	↓	8	10	8	10	↓	18	15	9	15	27
	100	↓	↓	13	9	13	9	↓	NS	21	14	21	14
713C	8	NS	NS	8	NS	8	NS	NS	NS	23	NS	23	NS
	24	↓	↓	9	16	9	16	↓	↓	40	35	40	35
	48	↓	↓	11	15	11	15	↓	↓	37	49	37	49
	72	↓	↓	17	13	17	13	↓	↓	39	55	39	55
	100	↓	↓	16	14	16	14	↓	28	45	61	45	89
738X	8	NS	NS	16	17	16	17	NS	26	39	67	39	93
	24	↓	31	17	12	17	43	↓	57	47	111	47	168
	48	↓	49	28	25	28	74	↓	89	61	128	61	217
	72	↓	65	39	34	39	99	↓	98	73	167	73	265
	100	↓	25	60	55	60	80	↓	100	120	222	120	322

[a] Isothermal for indicated test time.

[b] 1-Hour heating cycles for indicated test time.

[c] Value considered nonsignificant (if less than 1.5 sigma units) and not used to derive $\Delta\bar{t}_{total}$.

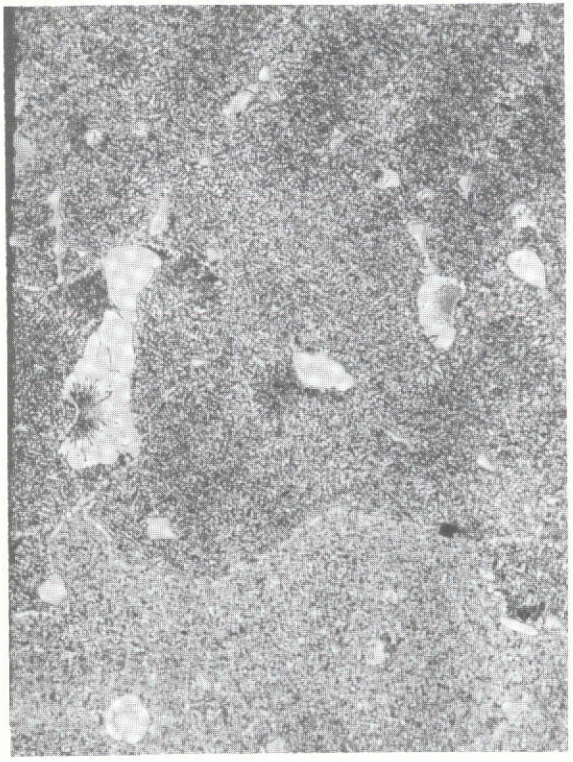

(a) Alloy VIA.

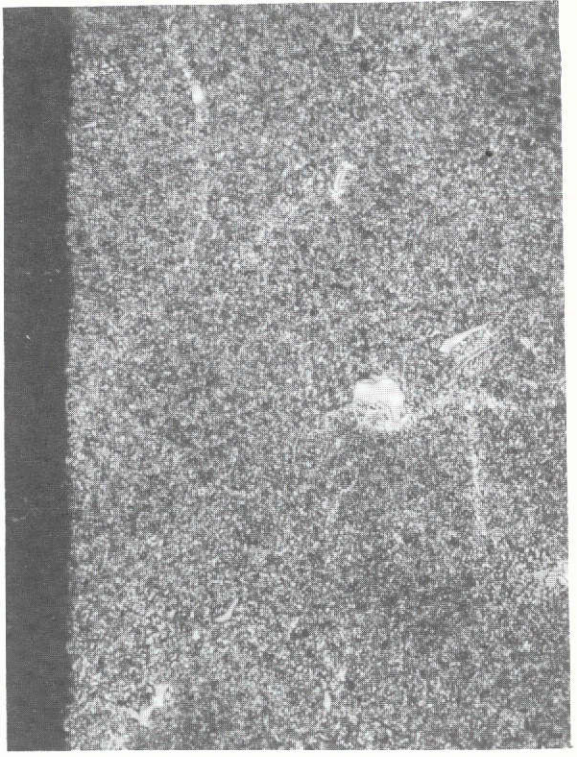

(b) Alloy B-1900.

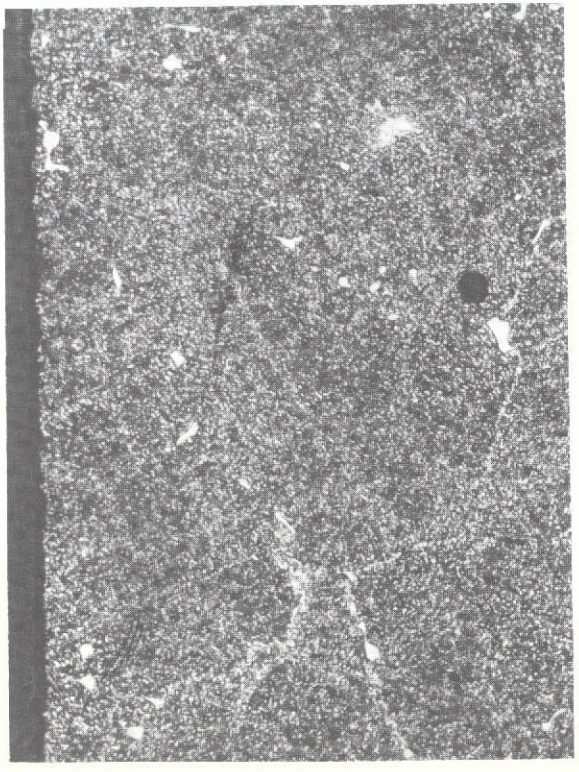

(c) Alloy 713C.

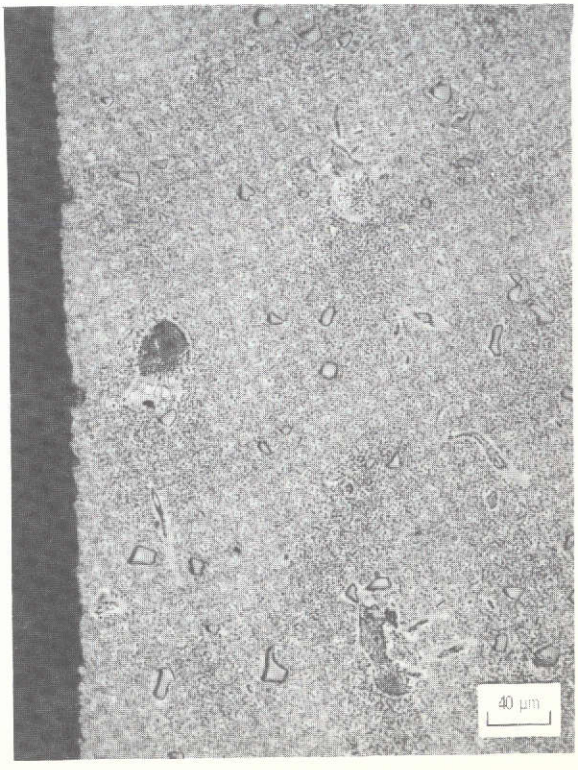

(d) Alloy 738X.

Figure 1. - Cross-sectional microstructures of as-cast alloys. Surface on left. Etchant: 33 water, 33 nitric acid, 33 acetic acid, and 1 hydrofluoric acid. X250.

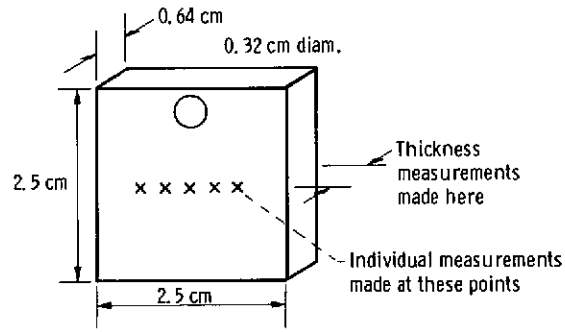

Figure 2. - Sample geometry and measurement of original thickness.

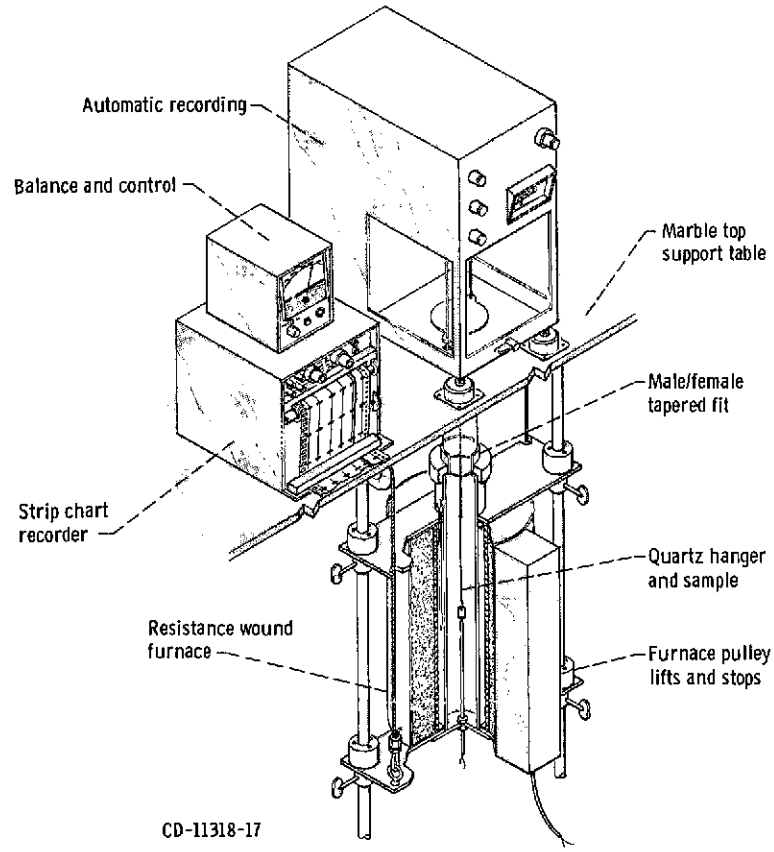

(a) Isothermal.

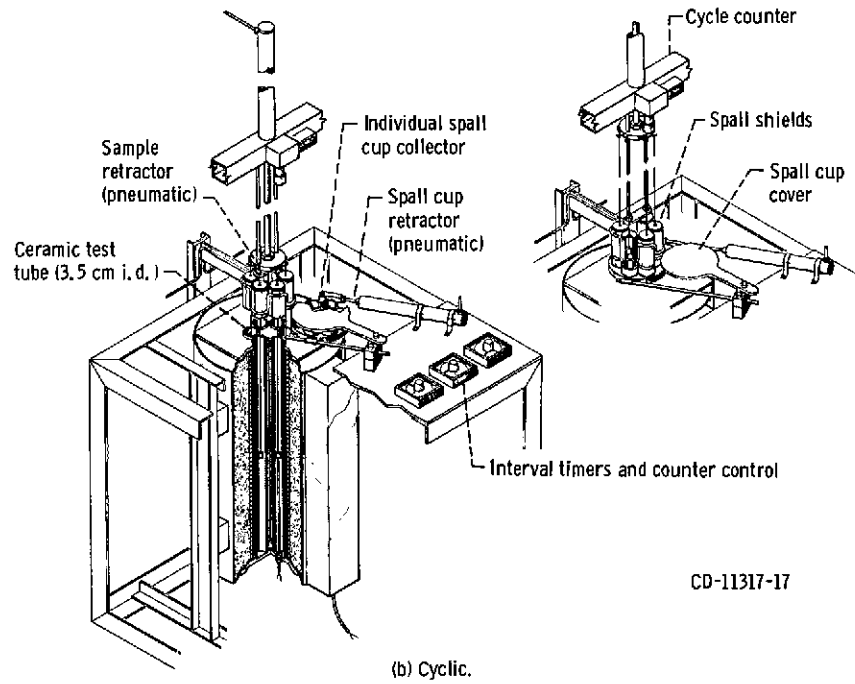

(b) Cyclic.

Figure 3. - Oxidation apparatus.

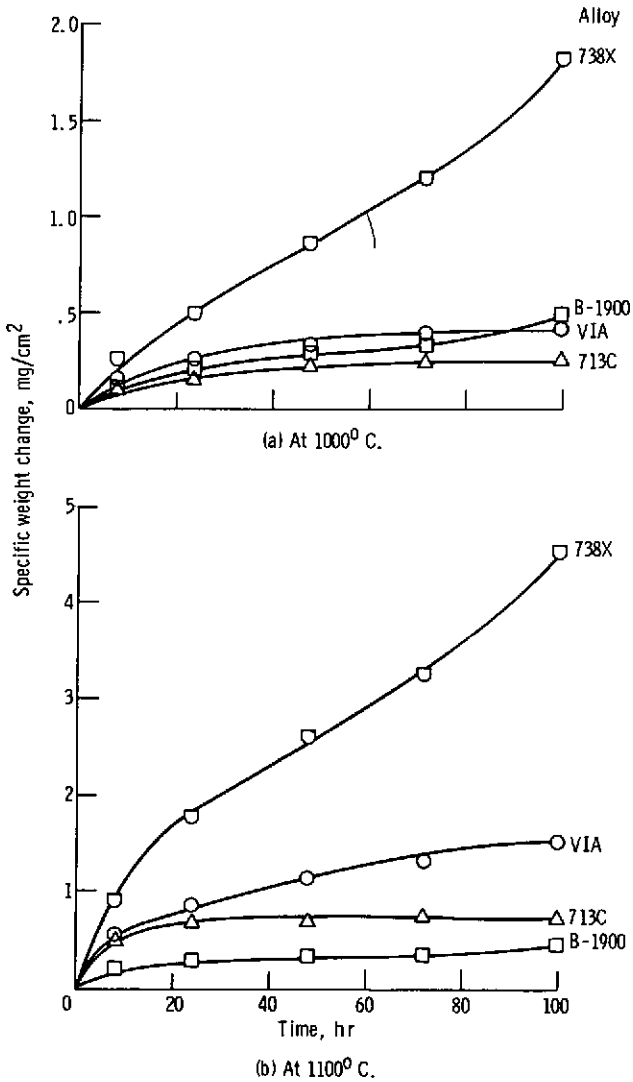

Figure 4. - Comparison of isothermal oxidation of four superalloys at 1000° and 1100° C in still air.

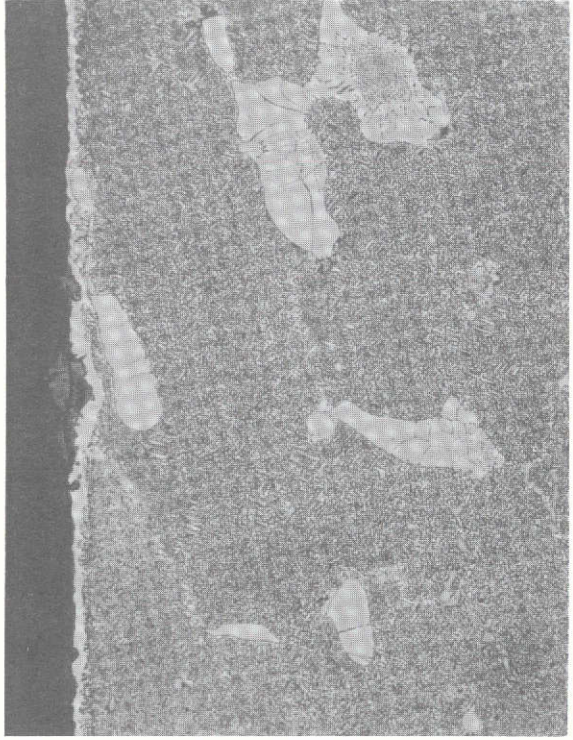

(a) Alloy VIA; 1000° C.

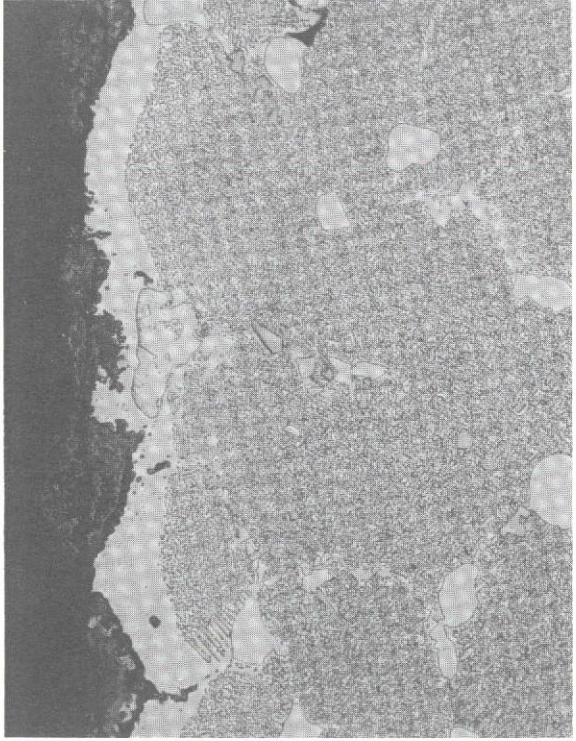

(b) Alloy VIA; 1100° C.

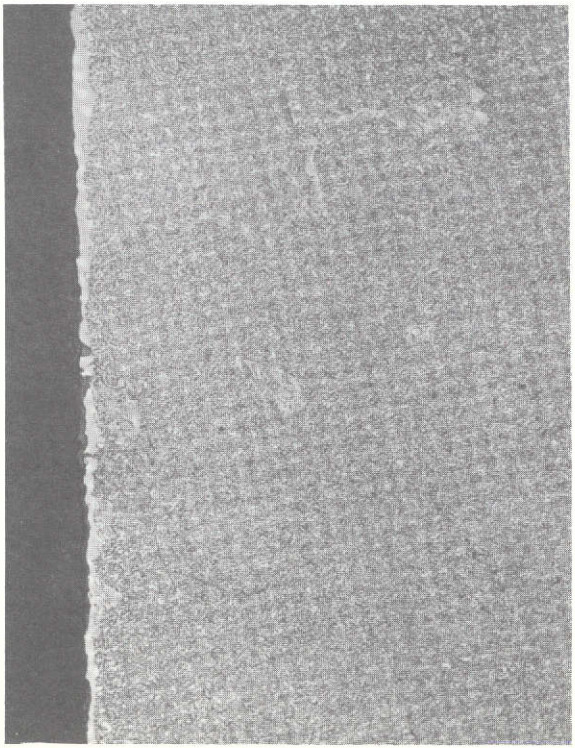

(c) Alloy B-1900; 1000° C.

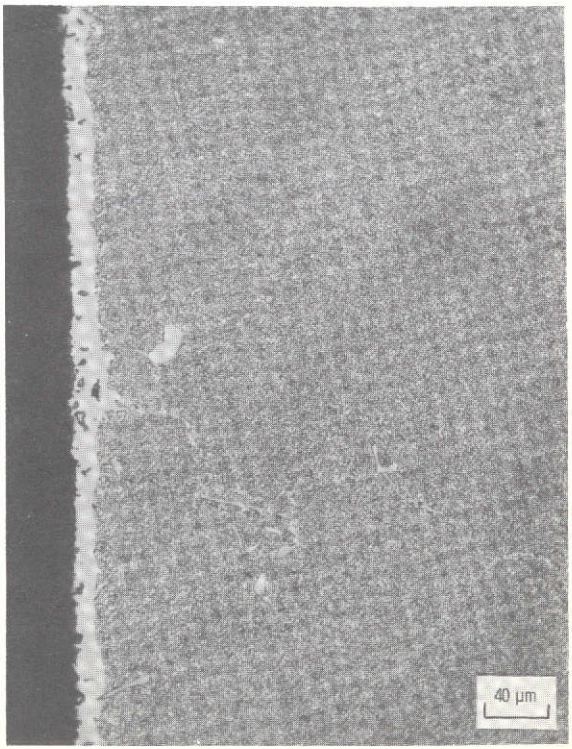

(d) Alloy B-1900; 1100° C.

Figure 5. - Microstructures of cross sections of test samples after 100 hours of isothermal oxidation at 1000° and 1100° C in still air. White depletion zone on left in each photograph. Etchant: 33 water, 33 acetic acid, 33 nitric acid, and 1 hydrofluoric acid. X250.

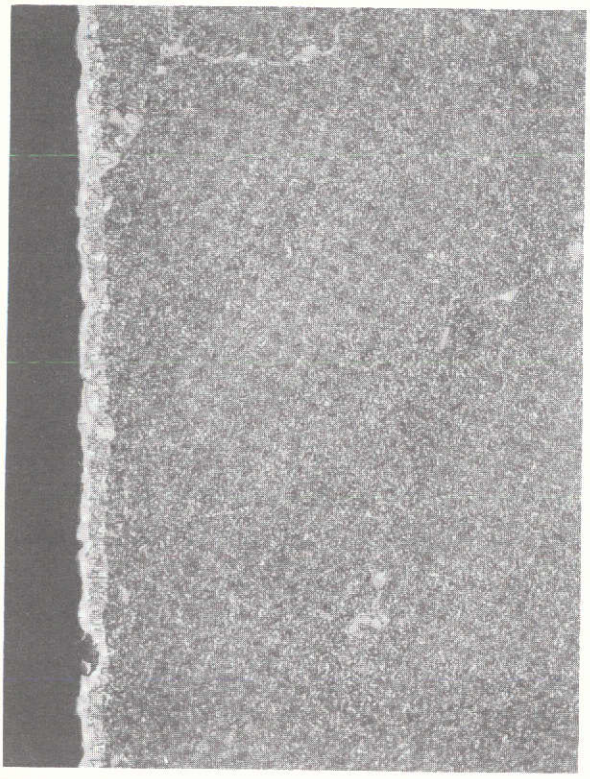

(e) Alloy 713C; 1000° C.

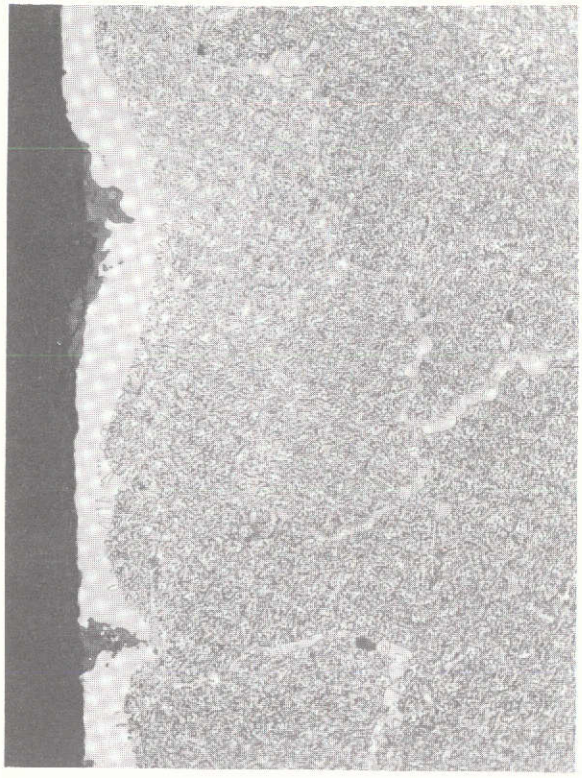

(f) Alloy 713C; 1100° C.

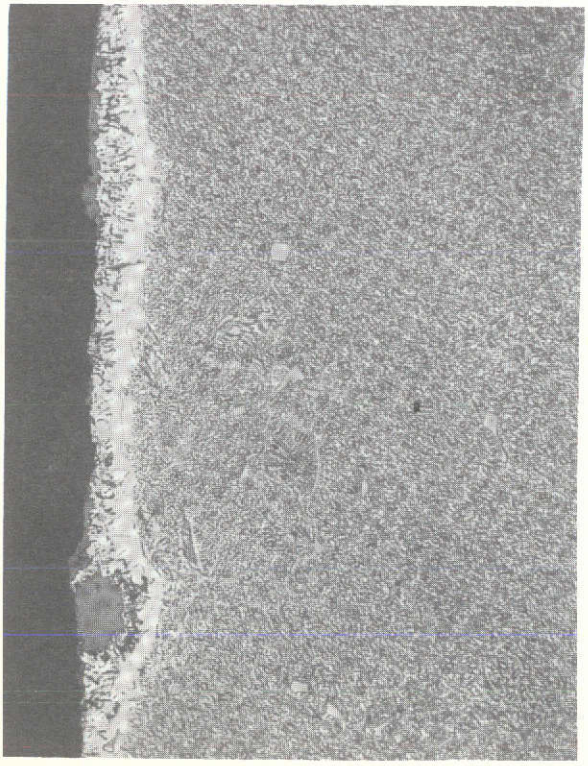

(g) Alloy 738X; 1000° C.

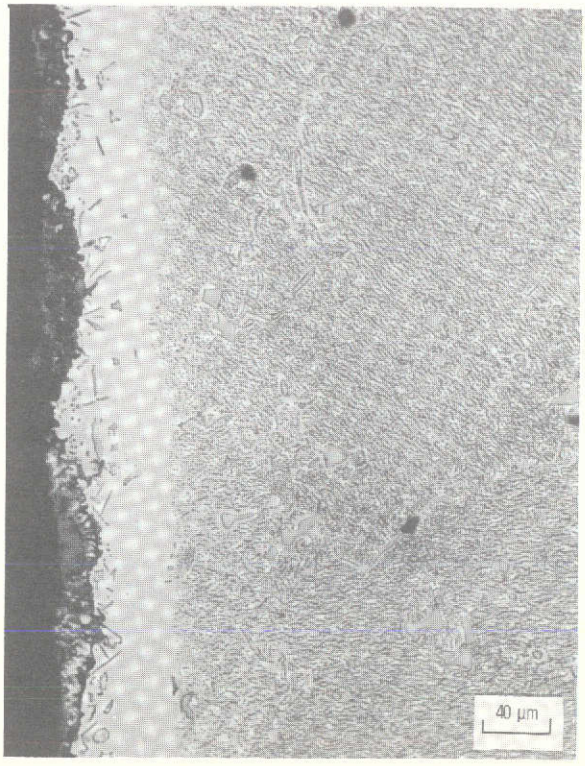

(h) Alloy 738X; 1100° C.

Figure 5. - Concluded.

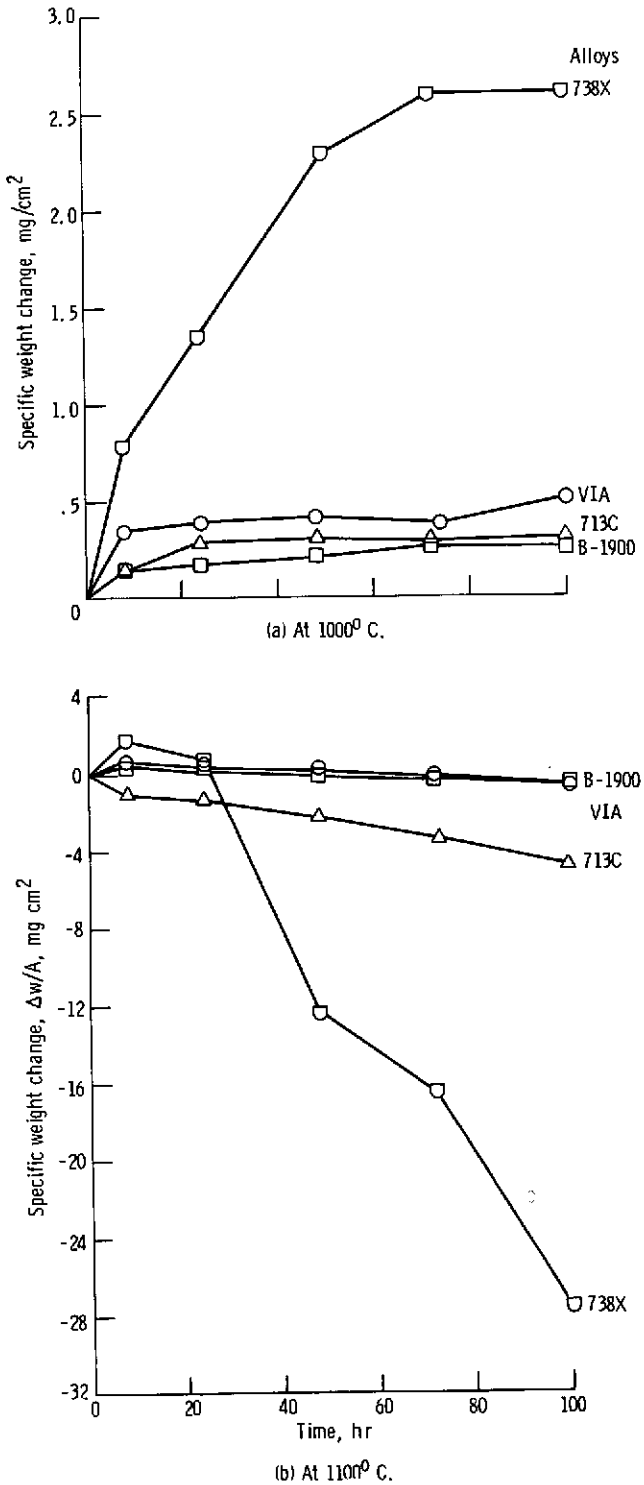

Figure 6. - Comparison of cyclic oxidation resistance of four superalloys at 1000^0 and 1100^0 C in still air for 1-hour heating cycles.

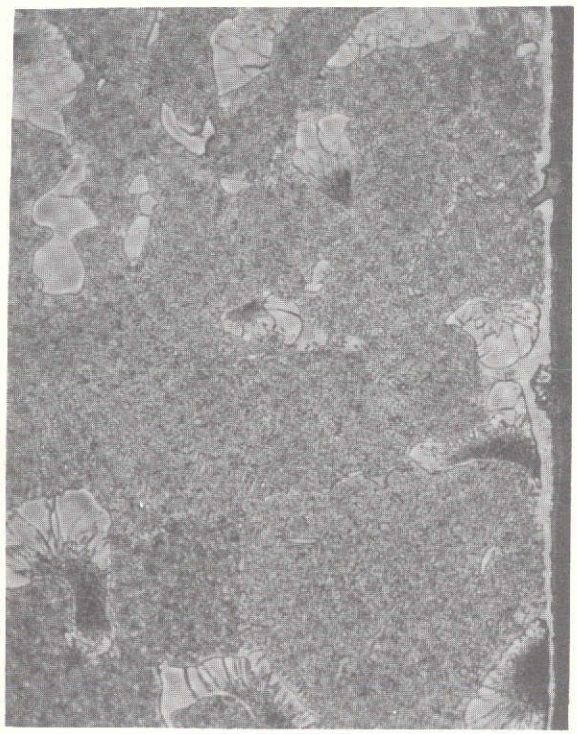

(a) Alloy VIA; 1000° C.

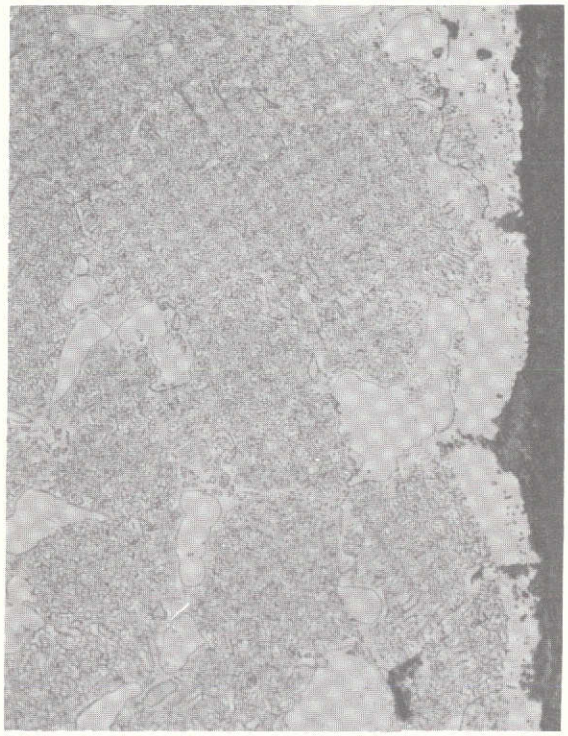

(b) Alloy VIA; 1100° C.

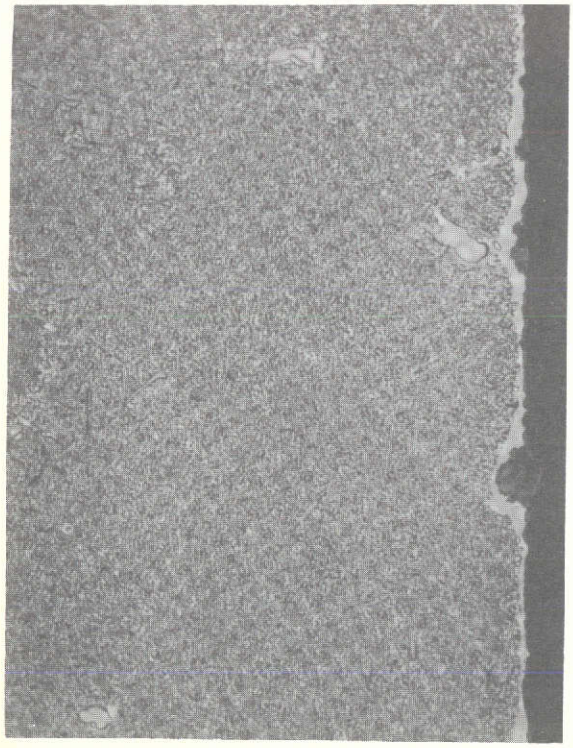

(c) Alloy B-1900; 1000° C.

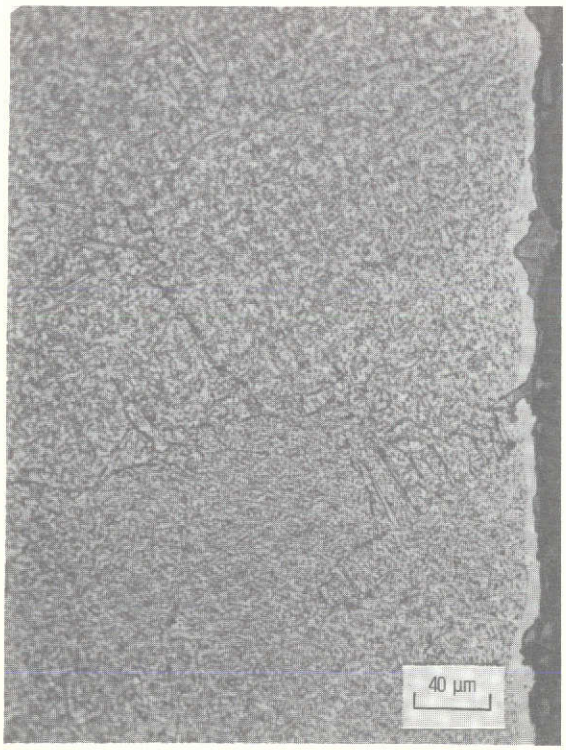

(d) Alloy B-1900; 1100° C.

Figure 7. - Microstructures of cross sections of test samples after 100 one-hour heating cycles at 1000° and 1100° C in still air. White depletion zone on right in each photograph. Etchant: 33 water, 33 acetic acid, 33 nitric acid, and 1 hydrofluoric acid. X250.

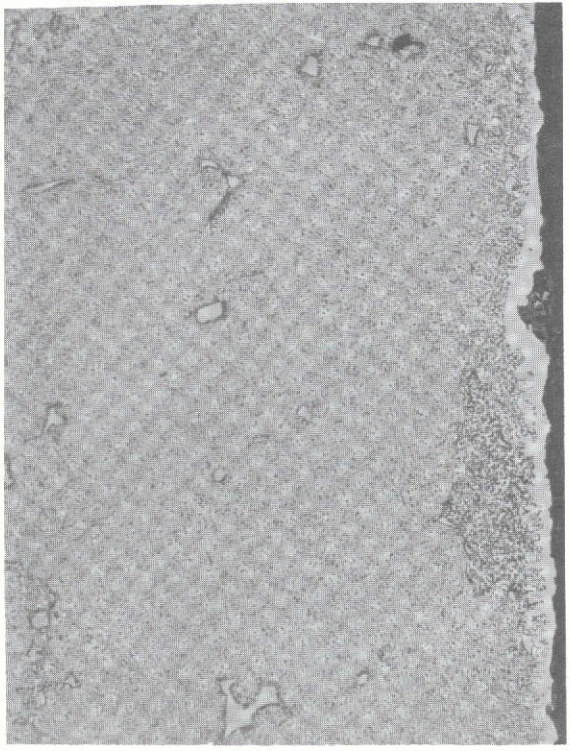

(e) Alloy 713C; 1000° C.

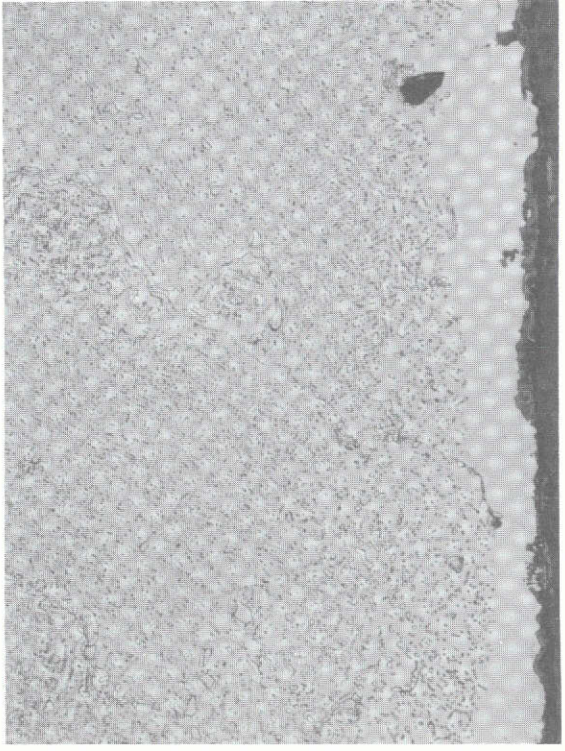

(f) Alloy 713C; 1100° C.

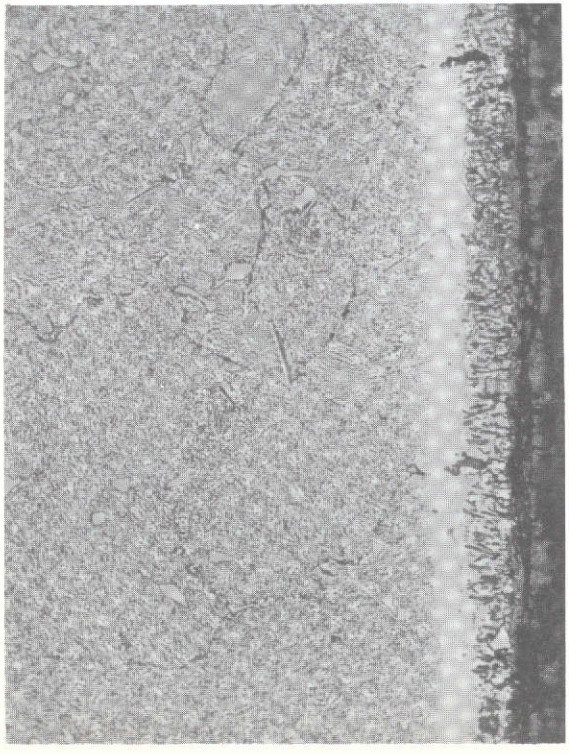

(g) Alloy 738X; 1000° C.

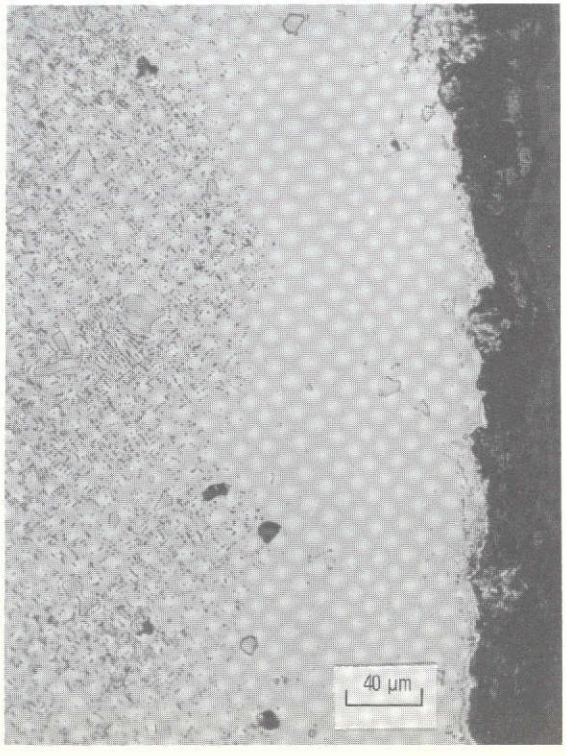

(h) Alloy 738X; 1100° C.

Figure 7. - Concluded.

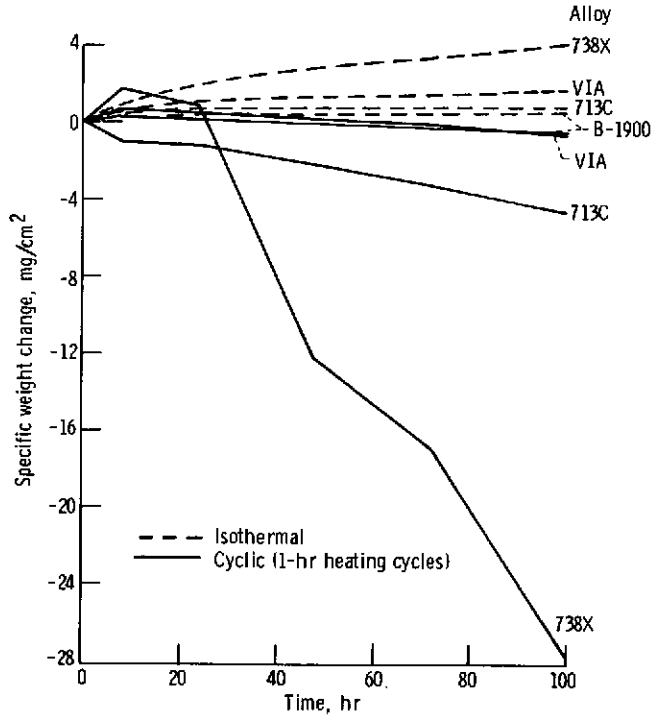

Figure 8. - Comparison of cyclic and isothermal oxidation at 1100° C in still air.